Physics Letters B 718 (2013) 931–936

Contents lists available at SciVerse ScienceDirect

Physics Letters B

www.elsevier.com/locate/physletb

Role of the cluster structure of ^{7}Li in the dynamics of fragment capture

A. Shrivastava [a,*], A. Navin [b], A. Diaz-Torres [c], V. Nanal [d], K. Ramachandran [a], M. Rejmund [b], S. Bhattacharyya [e], A. Chatterjee [a], S. Kailas [a], A. Lemasson [b], R. Palit [d], V.V. Parkar [a], R.G. Pillay [d], P.C. Rout [a], Y. Sawant [d]

[a] Nuclear Physics Division, Bhabha Atomic Research Centre, Mumbai 400085, India
[b] GANIL, CEA/DSM – CNRS/IN2P3, Bd Henri Becquerel, BP 55027, F-14076 Caen Cedex 5, France
[c] ECT*, Villa Tambosi, I-38123 Villazzano, Trento, Italy
[d] DNAP, Tata Institute of Fundamental Research, Mumbai 400005, India
[e] Variable Energy Cyclotron Centre, 1/AF Bidhan Nagar, Kolkata 700064, India

ARTICLE INFO

Article history:
Received 2 September 2012
Received in revised form 26 November 2012
Accepted 29 November 2012
Available online 1 December 2012
Editor: V. Metag

Keywords:
Particle-gamma coincidence
Weakly bound nuclei
Breakup fusion
Nuclear cluster structure
Classical dynamical model

ABSTRACT

Exclusive measurements of prompt γ-rays from the heavy-residues with various light charged particles in the ^{7}Li + ^{198}Pt system, at an energy near the Coulomb barrier ($E/V_b \sim 1.6$) are reported. Recent dynamic classical trajectory calculations, constrained by the measured fusion, α- and t-capture cross-sections have been used to explain the excitation energy dependence of the residue cross-sections. These calculations distinctly illustrate a two-step process, breakup followed by fusion, in case of the capture of t and α clusters; whereas for ^{6}He + p and ^{5}He + d configurations, massive transfer is inferred to be the dominant mechanism. The present work clearly demonstrates the role played by the cluster structures of ^{7}Li in understanding the reaction dynamics at energies around the Coulomb barrier.

© 2012 Elsevier B.V. All rights reserved.

In weakly bound nuclear systems, correlation among nucleons and pairing are manifested, among others, as an emergence of strong clustering and exotic shapes. This has renewed interest in the understanding of clusters based on concepts of molecular physics and the role of cluster states in nuclear synthesis [1,2]. Lithium isotopes present a unique example of nuclear clustering, with lighter isotopes (^{6,7}Li) having a well-known $\alpha + x$ cluster structure and the heaviest bound isotope (^{11}Li) exhibiting a two neutron Borromean structure. ^{9}Li has also been described as ^{6}He + t in a recent work [3]. ^{7}Li is an equally interesting case with its well-known weakly bound $\alpha + t$ structure ($S_{\alpha/t} = 2.47$ MeV), as well as less studied more strongly bound clusters ^{6}He + p ($S_{^{6}\mathrm{He}/p} = 9.98$ MeV) and ^{5}He + d ($S_{^{5}\mathrm{He}/d} = 9.52$ MeV) [4,5].

Recent studies with weakly bound nuclei have also focused on the understanding of the role of novel structures in the reaction dynamics [6]. Dominant reaction modes in nuclei with low binding energies, involve inelastic excitation to low-lying states in the continuum or transfer/capture of one of the cluster fragments from their bound/unbound states to the colliding partner nucleus [6–8]. The role of inelastic excitation of low-lying unbound states and transfer in the fusion hindrance, observed at energies well below the barrier, is also a topic of current interest [9,10]. When the capture occurs from unbound states of the projectile, the process could be looked upon as a two-step process, breakup followed by fusion (*breakup fusion*) [11–13]. In case of well-bound nuclei, nuclear reaction related to capture of heavy fragments by the target has been identified as incomplete fusion or massive transfer [14] and occurs predominately at energies $\geqslant$10 MeV/A. For weakly bound cluster nuclei such as ^{6,7}Li, the former has been shown to be important both above and at energies much below the Coulomb barrier [10,15]. Earlier studies have found the process of breakup fusion to be more dominant over a one step transfer in case of ^{6}Li(^{7}Li) for deuteron (triton) capture reaction [11–13].

A number of theoretical approaches for understanding the incomplete fusion process have been developed, as recently reviewed in [16–18]. These span a range of concepts and considerations, including breakup fusion, angular momentum window for incomplete fusion, promptly emitted particles, Fermi-jet, exciton, and moving source, thereby explaining the measured energy spectra and angular distribution of the emitted fragments and population of angular momentum in the compound system. Recently a theoretical description of breakup fusion for weakly bound nuclei has been incorporated in the three-dimensional classical trajectory model [7], considering the peripheral nature of the process

* Corresponding author.
E-mail address: aradhana@barc.gov.in (A. Shrivastava).

0370-2693/$ – see front matter © 2012 Elsevier B.V. All rights reserved.
http://dx.doi.org/10.1016/j.physletb.2012.11.064

for predicting both the spin distribution and sharing of excitation energy. The model treats the breakup process stochastically and follows the time evolution of individual fragments for a unique identification of reaction processes. More recently it has been improved to include the time propagation of the surviving breakup fragment and the breakup fusion product, allowing the description of their asymptotic angular distribution [8]. In contrast to most existing models for incomplete fusion, the new approach [7,8] treats the dynamics of incomplete fusion and provides a number of differential cross-sections that are critical for understanding exclusive experimental data. Such a theoretical model now allows for the first time to interpret data from exclusive experiments, which was not possible earlier.

The present work is aimed at exploiting the above model [7,8] to understand the dynamics of the process of fragment capture for the various cluster structures ($\alpha+t$, ^{6}He$+p$ and ^{5}He$+d$) of ^{7}Li, using exclusive particle-gamma coincidences to uniquely identify the source of the various residues formed. Integrated cross-sections of compound-nuclear fusion, t- and α-capture using both off- and in-beam gamma decay along with yields of the evaporation residues for different excitation energies of the composite system are reported. These results are compared with those of the recent three-dimensional classical trajectory model [7,8] in conjunction with the statistical model of compound-nucleus evaporation. This comparison demonstrates for the first time the important role played by the cluster structures of ^{7}Li in interpreting the dynamics of fragment capture.

Two independent experiments were performed at the 14UD pelletron Facility-Mumbai: a) Measurement of the prompt γ-rays from the heavy-residues in coincidence with various light particles α, t, d and p. The α-capture cross-sections were measured employing in-beam gamma method. b) Measurement of the excitation function for fusion, t-capture and neutron transfer using radioactive decay of the residues.

The measurements for exclusive in-beam γ decay of the residues were performed using a ^{7}Li beam of energy 45 MeV, incident on a 1.3 mg/cm^2 thick self supporting foil of ^{198}Pt with a 95.7% enrichment. Four telescopes (ΔE $\sim$ 25–30 μm and E $\sim$ 1 mm) at 50°, 60°, 120° and 130° (covering the region near and away from the grazing angle) were used to measure the charged particles. Four efficiency calibrated Compton suppressed clover detectors, operated in an add-back mode, were placed at 14.3 cm from the target at angles of 35°, −55°, 80°, and 155°. A coincidence between any charged particle recorded in the ΔE and a γ-ray in any clover detector or a two fold γ-ray coincidence between clover detectors was used as the master trigger. The reaction products arising from different channels were identified by their characteristic γ-ray transitions in coincidence with the outgoing particles. In the following we discuss the γ-ray spectra obtained by selecting different ejectiles recorded in the telescopes placed at 50° and 60° that cover region around the grazing angle. At backward angles, the contribution from fragment capture reaction was verified to be negligible.

Plotted in Fig. 1a is the γ-ray spectrum gated by the outgoing tritons with kinetic energy between 10 to 20 MeV, showing peaks from the residues of the composite system, ^{202}Hg, corresponding to capture of α-particles by the ^{198}Pt target. The γ-ray transitions from yrast-bands of ^{200}Hg, as reported in Ref. [19] for $\alpha + {}^{198}$Pt system, are observed. In case of ^{199}Hg, the γ-ray transitions feeding the long lived isomeric state ($13/2^+$, $T_{1/2} \sim 42.8$ min), known from an earlier study in $\alpha + {}^{198}$Pt system [20] are labeled. The triton spectrum from the two telescopes was further divided into smaller energy bins (2.5 MeV) to study the variation in population of the residues as function of triton energy and is shown in Fig. 1b. The γ-ray spectra related to the two bins are plotted as

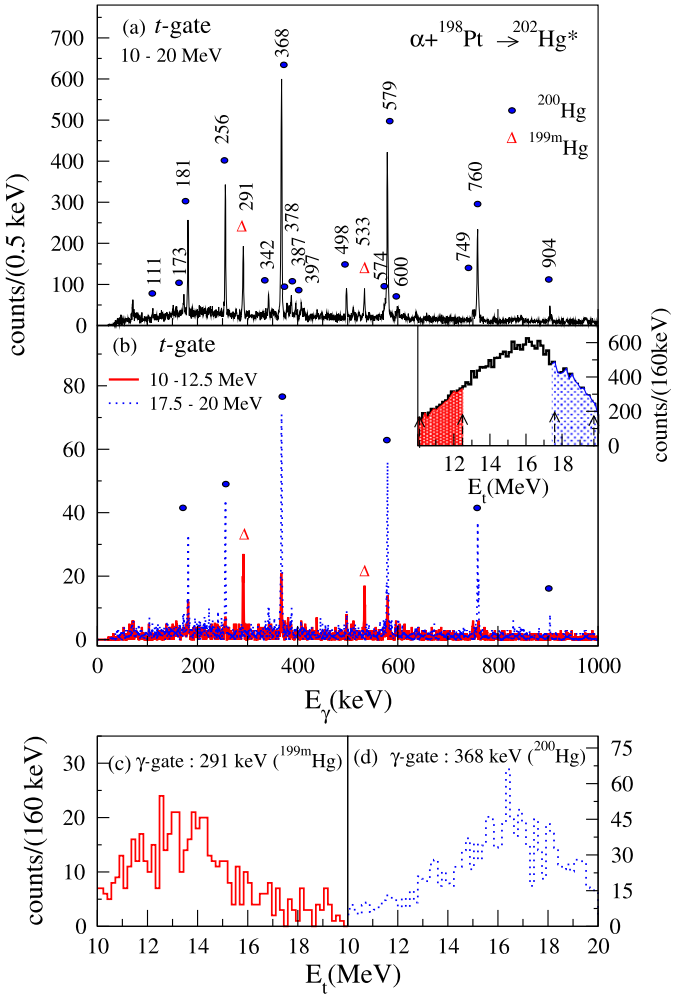

Fig. 1. (Color online.) (a) Prompt γ-ray spectra obtained in coincidence with outgoing t (α-capture) having an energy 10 to 20 MeV. (b) same as (a) but subdivided into two different energy bins of the t (10 to 12.5 MeV and 17.5 to 20 MeV as shown in the inset). (c) and (d) Triton energy spectrum at 50°, in coincidence with 291 keV and 368 keV γ-rays arising from transitions in ^{199}Hg and ^{200}Hg respectively.

solid and dotted curves. The outgoing tritons with higher (lower) kinetic energy correspond to lower (higher) excitation energy deposited in ^{202}Hg. As can be seen from the figure the γ-peaks of the residues corresponding to the two neutrons evaporation channel (^{200}Hg) are dominant with the higher triton energy bin while those from three neutron evaporation channel (^{199}Hg) are dominant with the lower energy bin. A similar conclusion can be obtained from Figs. 1c, d that show triton spectra obtained by selecting the 291 keV and 368 keV γ-ray transitions from ^{199}Hg and ^{200}Hg respectively. The relative population of ^{200}Hg corresponding to each bin of the triton spectrum were estimated from the efficiency corrected yields of γ-ray transition to the ground state. A similar procedure was followed for ^{199}Hg for transitions above the isomeric state, $13/2^+$ at 532 keV.

In Fig. 2a, the γ-ray spectrum obtained in coincidence with α-particles shows contribution arising from different reaction channels. The main γ-ray transitions in the spectrum arise from ^{198,199}Au [21] (residues due to t-capture). Shown in Figs. 2b, c are the γ-ray spectrum in coincidence with the deuterons and protons respectively. Comparing these spectra with Fig. 1a, it can be noticed that more neutron rich residues (due to capture of the heavier complementary particle), are populated in going from spectra in coincidence with t to p. In the γ-ray spectrum gated

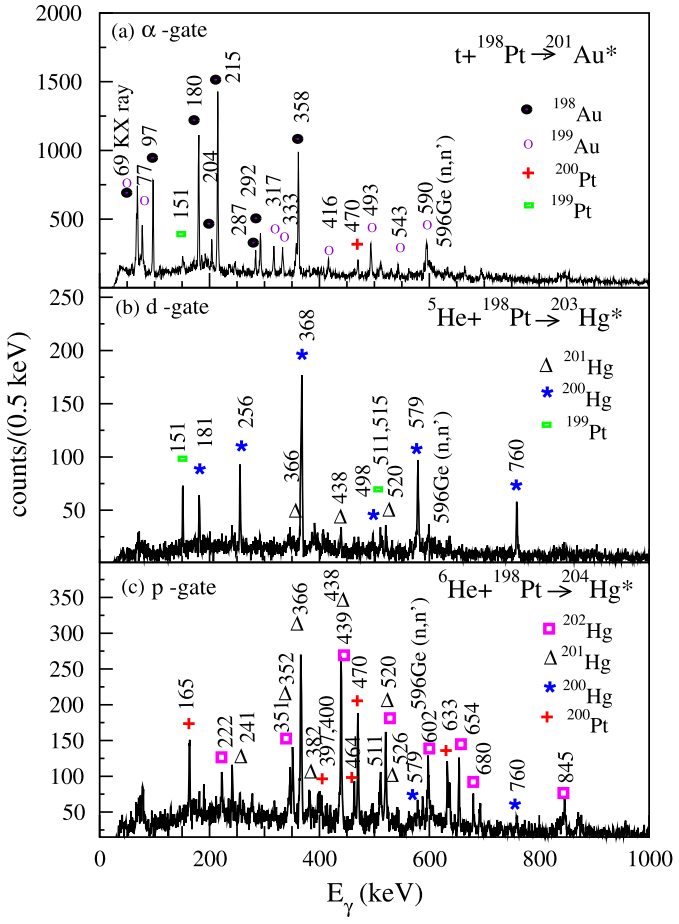

Fig. 2. (Color online.) In beam γ-ray spectra in coincidence with outgoing fragments (a) α, (b) d and (c) p. The gamma transitions from the residues populated from capture of t, ^{5}He and ^{6}He are indicated in (a)–(c) respectively. The γ-rays arising from 1n- and 2n-transfer (^{199,200}Pt) are also labeled.

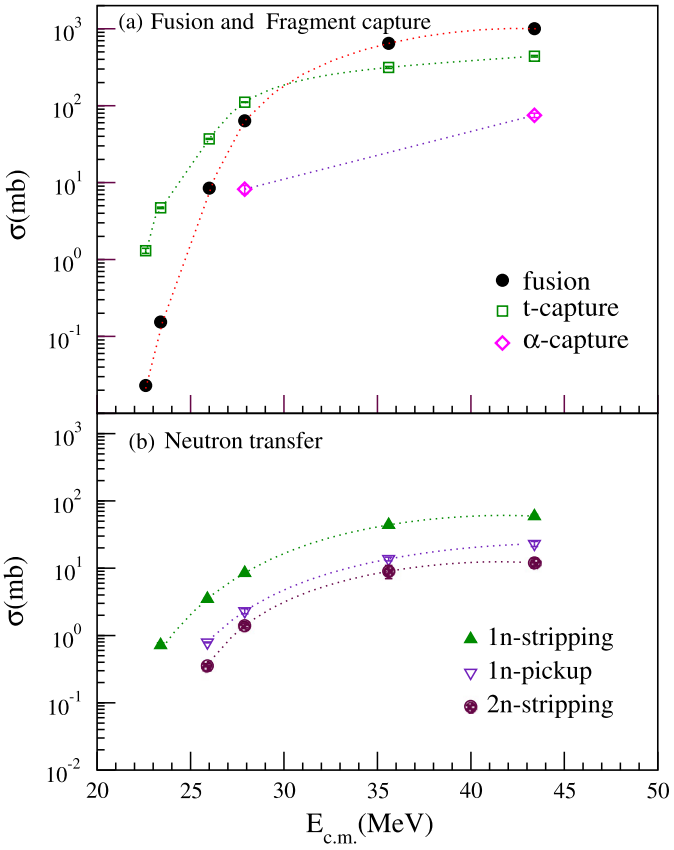

Fig. 3. (Color online.) Integrated cross-sections for (a) compound-nuclear fusion ($^{199-202}$Tl), t-capture ($^{198-200}$Au) and α-capture ($^{199-200}$Hg), (b) neutron transfer corresponding to 1n-pickup (^{197}Pt) and 1n-, 2n-stripping (^{199,200}Pt) reactions. The dashed lines in panels (a) and (b) are to guide the eye.

by the deuterons, the peaks arise mainly from the residues that can be attributed to decay of ^{203}Hg arising from the capture of ^{5}He (Fig. 2b). The known γ-ray transitions from ^{200,201}Hg could be identified. The dominant peaks observed in Fig. 2c are from the ^{201,202}Hg residues, of the composite system ^{204}Hg formed after capture of ^{6}He.

The γ-ray transitions from ^{199,200}Pt, corresponding to one and two neutron transfer reactions are observed in the α, d and p gated spectra. This can be understood as follows. The ejectile resulting from one neutron transfer (^{6}Li) has no bound excited state. The excited states populated in the continuum of ^{6}Li after transfer of a neutron, disassociate into $\alpha + d$ [22]. These events are identified from the characteristic γ-ray transitions of ^{199}Pt observed in coincidence with d (Fig. 2b). Spectroscopy information for ^{199}Pt is presently limited. The unidentified peak at 151 keV has been tentatively assigned to ^{199}Pt since this γ-ray transition was also observed in coincidence with ^{6}Li. The γ-ray transitions from ^{200}Pt observed in coincidence with p in Fig. 2c are attributed to the breakup of excited unbound states in ^{5}Li into $\alpha + p$ after transfer of two neutrons. In the α gated spectrum (Fig. 2a), peaks arising from ^{199,200}Pt are small compared to dominant peaks arising from residues from t-capture, which are formed with relatively larger cross-sections. This was confirmed from the offline-measurement of the neutron transfer and t-capture cross-sections (as shown in Fig. 3 and discussed below).

The peaks at 366 keV and 241 keV in Fig. 2c could not be identified among the known transitions of ^{200,201,202}Hg and ^{200}Pt. A probable candidate could be from the decay of states above the $13/2^{+}$ isomer in ^{201}Hg. No spectroscopy information of the prompt gamma transition above this state is presently available in literature. Change in γ-ray intensity of these transitions as compared to transitions from ^{202}Hg was studied with different energy bins of the scattered proton, further confirming this assignment to ^{201}Hg. This observation shows advantage of the breakup fusion reaction for studying nuclear states at higher spin, not accessible by the compound-nuclear fusion, earlier demonstrated in Ref. [23].

The cross-section of the residues, ^{199}Hg and ^{200}Hg from α-capture were deduced by performing coincidence between γ-ray transitions from the yrast-band built on ground state in case of ^{200}Hg and on the isomeric state ($13/2^{+}$) in case of ^{199m}Hg. The coincidence condition improved the quality of the spectra especially for the peaks that could not be resolved from the peak of interest. The cross-section for ^{199m}Hg was also obtained by following the radioactive decay of the isomeric state ($13/2^{+}$). This was found to be in a good agreement with the value extracted from the in-beam method. The α-capture cross-sections, obtained by adding cross-section of ^{199m}Hg and that of ^{200}Hg are shown in Fig. 3a at beam energies of 29 and 45 MeV.

The measurement of the cross-section of the residues resulting from the process of fusion, t-capture and neutron transfer channels were performed with beams of ^{7}Li in the range of 22 to 45 MeV incident on self supporting foils of ^{198}Pt target (95.7% enriched, ~1.3 mg/cm^2 thick) followed by an Al catcher foil of thickness ~1 mg/cm^2. Two efficiency calibrated HPGe detectors with Be window were used in a low background counting setup with graded shielding for off-beam gamma ray measurements. The

Table 1
PLATYPUS calculation for integrated α-capture, t-capture and complete fusion cross-sections in ^{7}Li + ^{198}Pt [24] at a beam energy of 45 MeV.

Reaction channel	σ expt. (mb)	σ PLATYPUS (mb)
α-capture	75 ± 5	77
t-capture	440 ± 10	366
complete fusion	1004 ± 50	958

Table 2
Woods–Saxon potentials employed in the ^{7}Li + ^{198}Pt PLATYPUS calculation. The strength V_0 is in MeV, while the radius r_0 and diffuseness a_0 parameters are in fm.

Mass partitions	(V_0, r_0, a_0)
^{7}Li + ^{198}Pt	(−41.58, 1.640, 0.630)
α + ^{198}Pt	(−10.26, 1.534, 0.587)
t + ^{198}Pt	(−26.40, 1.562, 0.595)
$t + \alpha$	(−18.16, 1.284, 0.630)
t + ^{202}Hg	(−26.40, 1.562, 0.590)
α + ^{201}Au	(−10.26, 1.534, 0.584)

residues in case of fusion ($^{199–202}$Tl) were identified by using KX-γ-ray coincidence of the decay radiations from the irradiated sample with detectors placed face to face. Further details of the setup can be found in Refs. [10,24].

The γ-ray yields for residues formed after t-capture ($^{198–200}$Au) and for target-like nuclei after neutron transfer (^{197,199,200}Pt) were extracted from inclusive γ-ray measurements. The t-capture and fusion cross-sections were obtained by taking the sum of individual measured evaporation residue cross-sections. The excitation function for fusion, fragment capture and neutron transfer reactions are plotted in Figs. 3a, b; respectively. Corrections for ^{196}Pt impurity in the target (2.56%) were found to be negligible (<1%). The error on the cross-section arises mainly from statistics. Other sources of error in the cross-sections, arising from the uncertainties in measurements of the beam current, γ-ray efficiency, target thickness and available spectroscopic information of the residues were estimated to be between 10 to 15%. The cross-sections for fusion and fragment capture at the highest energy (45 MeV) are also listed in Table 1.

A three-body classical dynamical model [7,8] implemented in the PLATYPUS code [25] allows a consistent analysis of breakup, incomplete, and complete fusion processes. The measured integrated cross-sections of complete fusion, α-capture and t-capture for the ^{7}Li + ^{198}Pt system at 45 MeV (Fig. 3a and Table 1) were used to constrain the parameters of the model while predicting the differential cross-section as a function of excitation energy and angular momentum for the formation of the primary composite system. These differential cross-sections are the key inputs to the statistical model code PACE2 [26] for calculating the cross-section of evaporation residues from decay of the composite system.

The PLATYPUS calculations were carried out considering ^{7}Li as $\alpha + t$ cluster, having a binding energy of 2.47 MeV. In this calculation breakup fusion occurs when any of the breakup fragment (α or t) penetrates the Coulomb barrier between the fragment and the target. Complete fusion occurs when the entire projectile, ^{7}Li or both α and t get captured inside the interaction barriers. Parametrization of the Coulomb and nuclear potential was same as in Ref. [7]. The pre- and post-breakup Coulomb and nuclear interactions between the participants (^{7}Li + ^{198}Pt, α + ^{198}Pt, t + ^{198}Pt, $t + \alpha$, t + ^{202}Hg and α + ^{201}Au), were taken as those between a point charge and a spherical distribution for the heaviest fragment ($=1.2A^{1/3}$). The nuclear interaction was parametrized by a Woods–Saxon potential (Table 2) which provided Coulomb barriers similar to those of the Sao Paulo potential [27].

Parameters necessary for the breakup-probability function [$A\exp(-\beta R)$, where R denotes the internuclear distance] were obtained by reproducing the measured integrated cross-section of t-capture and α-capture and the complete fusion for ^{7}Li + ^{198}Pt (Table 1). The amplitude and slope of the breakup-probability function were $A = 1.68 \times 10^{4}$ and $\beta = 0.9$ fm^{-1}, respectively [8]. Location of the breakup of ^{7}Li into α and t was determined by Monte Carlo sampling of the breakup function up to $R = 50$ fm. The instantaneous dynamical variables of the excited projectile at the breakup point, namely its total internal energy ($E_{rel} \leqslant 6$ MeV), its angular momentum (up to 4$\hbar$), the fragment separation and their orientations, were also Monte Carlo sampled [8]. The cross-section for α- and t-capture were calculated using a sharp cut-off in angular momenta. The convergence of the calculated cross-section was ensured by including projectile-target partial waves up to 50$\hbar$, for a sample of 1000 projectiles per partial wave. The calculations were found to be in agreement with the shape of the measured energy spectrum of surviving α-particles and t. As the fusion barrier for t + ^{198}Pt is smaller than that for α + ^{198}Pt, the cross-section for t-capture is larger relative to α-capture. The comparison between the calculation and the measured values are shown in Table 1.

To get further insight into the mechanism of fragment capture, the measured yields of the evaporation residues obtained from the particle-gamma coincidence data were compared with the predictions from PLATYPUS + PACE2 for different excitation energies (E*) of the primary composite system as discussed below. The spectrum of the surviving α-particles, after capture of the complementary fragment (t), represents the cross-section for breakup fusion as a function of the kinetic energy of the α-particles (E_α). This can be expressed as a function of E* of the composite system ^{201}Au, by obtaining the E* for each value of E_α, using the dynamical variables at the instant of breakup of ^{7}Li into $\alpha + t$ on an event by event basis. The calculated E* and the corresponding breakup fusion cross-section as a function of spin (σ_J vs. J) were given as input to the statistical model code PACE2 [26] for calculating the evaporation residue cross-sections from decay of ^{201}Au formed after triton-fusion. The calculated values of absolute cross-sections for the residues, ^{198,199}Au, are plotted as solid and dashed curves in Fig. 4a. The measured yields of ^{198}Au from the second bin (bin II in inset Fig. 3a) of α-particle spectrum, were normalized to the calculated cross-section obtained using PACE2 for the E* = 30 MeV that corresponds to the $E_\alpha = 24$ MeV (center of the bin used). The cross-section for ^{198,199}Au deduced after applying the same normalization to their respective yields in each bin (bin I, III and IV in inset of Fig. 3a) and are plotted in Fig. 4a. The errors on cross-sections are only statistical in nature. A reasonably good agreement is observed with the calculation. These results suggest that the main mechanism responsible for t-capture is fusion of t after breakup of ^{7}Li, as modeled in the PLATYPUS code. Following the same procedure, cross-sections for residues arising from the capture of α-particles for a given energy (corresponding to outgoing triton energy, inset of Fig. 4b) were calculated from PACE2, using spin distribution and excitation energy of ^{202}Hg obtained from PLATYPUS and are shown in Fig. 4b. The calculated cross-section of ^{200}Hg at E* = 27 MeV was used to normalize the measured yield of ^{200}Hg and ^{199}Hg. In case of ^{199}Hg the γ-ray transitions only above the $(13/2^{+})$ isomeric state were considered hence the measured cross-sections only provide a lower limit for this channel. The energy dependence of formation of both the residues agrees well with the statistical model calculations, showing a similar dominance of the breakup fusion process. The PLATYPUS calculations indicate that the breakup fusion process is dominated by breakup events with $E_{rel} \leqslant 4$ MeV,

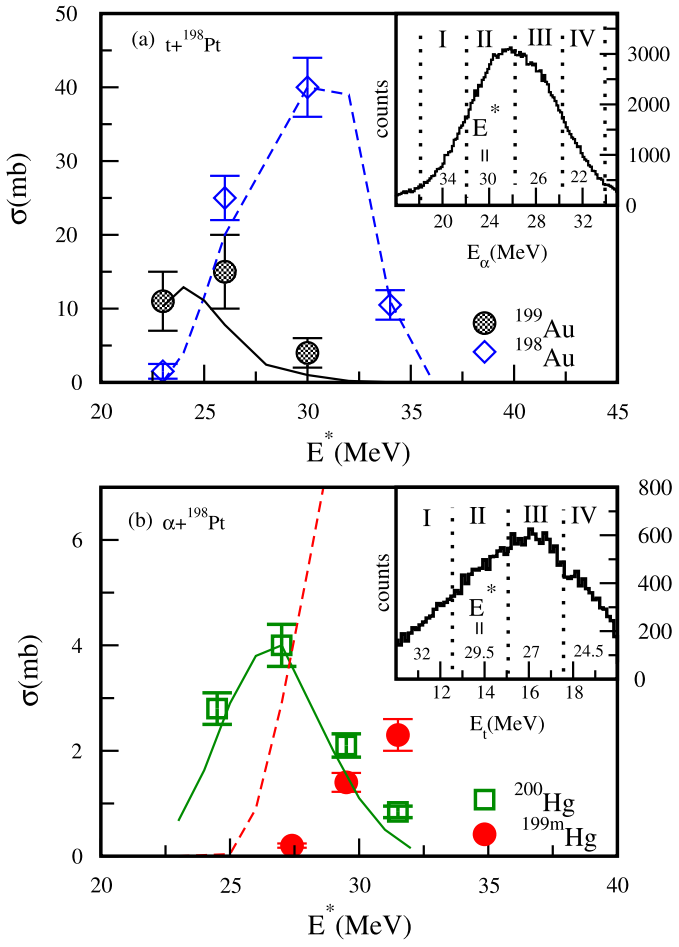

Fig. 4. (Color online.) (a) Residue cross-sections as a function of excitation energy (E^*) of the primary composite system formed after t-capture. The E^* in ^{201}Au, corresponding to kinetic energy (E_α) of the surviving α-particle (shown in the inset) is calculated from the classical trajectory model of breakup fusion – PLATYPUS. (b) same as (a) but for α-capture. The data points for ^{199}Hg (filled circle) represent the lower limit for the cross-sections for this channel as contributions below the isomeric state ($13/2^+$) are not included. The solid and dashed curves are statistical model calculations (PACE2) for two and three neutron evaporation channels, using the angular momentum distribution and excitation energy of the primary composite system obtained from PLATYPUS (see text). The residue cross-sections of (a) and (b), when summed over E^*, are equal to the integrated cross-section at a beam energy of 45 MeV as plotted in Fig. 3a for t- and α-capture respectively.

which only includes prompt breakup. This type of breakup is critical, as the resonant states have life time larger than the interaction time [28]. It can be noticed from the inset of Figs. 4a, b that both α and t spectra peak around the beam velocity, as expected from the breakup fusion model of PLATYPUS.

A similar analysis was attempted by modeling ^{7}Li as a cluster of ^{6}He + p (breakup threshold 9.975 MeV). The average E^* of the composite system ^{204}Hg computed using PLATYPUS is high (42 MeV) due to large positive Q-value (+12.4 MeV) for ^{6}He fusing with ^{198}Pt. The major residue channels predicted at this E^* and over the measured range of proton energies are ^{199,200}Hg. The γ-transitions for ^{199}Hg are not observed while those from ^{200}Hg are found to be populated weakly (with the proton gate). Multi-nucleon transfer reactions are known to take place preferentially at an optimum Q-value (Q_{opt}) obtained from the semi-classical trajectory matching condition [29]. The available E^* ($Q_{gg} - Q_{opt} = 31$ MeV) from transfer of ^{6}He (Table 3) is favorable for populating the residue channels ^{201,202}Hg, which is consistent with the present measurement (Fig. 2c). The same is

Table 3
Ground state Q-values for the α, t, ^{5}He and ^{6}He transfer channels observed in the ^{7}Li + ^{198}Pt along with optimum Q-values estimated from the semi-classical transfer trajectory matching condition. The excitation energies for breakup fusion from PLATYPUS calculation are also tabulated.

Exit channel	Q_{gg} (MeV)	Q_{opt} (MeV)	E^*_{PLATYPUS} (MeV)
$\alpha + ^{201}$Au	+8.9	−14.1	28.0
$t + ^{202}$Hg	−2.6	−28.6	25.5
$d + ^{203}$Hg	−2.8	−28.6	38.0
$p + ^{204}$Hg	+2.4	−28.6	42.0

found to be applicable for the ^{5}He + d cluster structure of ^{7}Li (breakup threshold = 9.522 MeV, fusion Q-value = +6.75 MeV). The average E^* calculated from PLATYPUS for this combination (Table 3) favors residue channels ^{198,199}Hg for which the γ-transitions are not visible in the d gated spectrum. While the lower E^* estimated from transfer Q-values is more suited for populating ^{200}Hg, in concurrence with the data (Fig. 4b). It is worth noting that, although not included in the present calculations, the unstable ^{5}He fragment (half-life of 7.6×10^{-22} s) can be dissociated into $\alpha + n$ near the ^{198}Pt target. Events where the alpha particle is captured and the neutron survives along with the deuteron might happen, forming the ^{202}Hg compound-nucleus with $E^* \sim 25$ MeV. These events compete with those involving the ^{7}Li binary fragmentation into $\alpha + t$, where the α-particle gets captured and the triton escapes. However, the latter component should be dominant based on the smaller breakup-threshold value, i.e., 2.47 MeV compared to 9.522 MeV.

Based on these observations it can be inferred that, for the capture of ^{5,6}He from the well-bound cluster configurations of ^{7}Li, the large value of the breakup threshold does not favor the process of breakup fusion, unlike that for the t- and α-particles that are weakly bound in ^{7}Li, and massive transfer from bound states could be the main process.

In summary, exclusive measurement of the outgoing particles and γ-rays in conjunction with the calculations made using a classical dynamical model have demonstrated for the first time, the critical role of different cluster structures of ^{7}Li in the dynamics of reaction mechanism. A good agreement between the calculations and the measured quantities suggests, the dominant mechanism of capture of the fragments with low binding energy in ^{7}Li (t and α) after the inelastic excitation of ^{7}Li above the breakup threshold is breakup followed by fusion. The low-lying states (up to 4 MeV) in the continuum populated by the direct breakup of ^{7}Li make the major contribution to the breakup fusion cross-section. In case of capture involving ^{5}He + d and ^{6}He + p clusters with relatively high binding energy in ^{7}Li, the evaporation residues are more neutron rich than predicted from the model for fusion of ^{5}He and ^{6}He after the breakup, suggesting that the mechanism is not breakup fusion but could be massive transfer.

The cross-section of evaporation residues for different excitation energies of the composite system, formed after fusion of t- and α-particles were successfully explained, by the classical dynamical model of breakup fusion. This information can be useful for studying nuclear structure of the nuclei formed as ^{5,6}He + target or t + target, using a ^{7}Li beam [30]. There are no existing quantum approaches for quantifying these measurements which are planned in rare isotope beam facilities. Although it is a great theoretical challenge, the development of such a quantum approach is highly desirable. The present results are useful for the theoretical developments, and also have implication in predicting production cross-section of exotic nuclei with radioactive ion beams for performing high spin spectroscopy. It would be interesting to extend

such studies with radioactive nuclei having predominant weakly bound cluster structures and to develop the classical dynamical model further.

Acknowledgements

We acknowledge the accelerator staff for smooth running of the machine. A.D.-T. thanks Leandro Gasques for providing him with Sao Paulo potential barriers.

References

[1] H. Horiuchi, K. Ikeda, K. Kato, Prog. Theor. Phys. Suppl. 192 (2012) 1.
[2] M. Freer, Rep. Prog. Phys. 70 (2007) 2149;
W. von Oertzen, M. Freer, Y. Kanada-En'yo, Phys. Rep. 432 (2006) 43.
[3] Y. Kanada-En'yo, T. Suhara, Phys. Rev. C 85 (2012) 024303.
[4] D.R. Tilley, et al., Nucl. Phys. A 708 (2002) 3.
[5] Z.H. Li, et al., Eur. Phys. J. A 44 (2010) 1.
[6] N. Keeley, R. Raabe, N. Alamanos, J.L. Sida, Prog. Part. Nucl. Phys. 59 (2007) 579;
N. Keeley, N. Alamanos, K.W. Kemper, K. Rusek, Prog. Part. Nucl. Phys. 63 (2009) 396.
[7] A. Diaz-Torres, et al., Phys. Rev. Lett. 98 (2007) 152701.
[8] A. Diaz-Torres, J. Phys. G: Nucl. Part. Phys. 37 (2010) 075109.
[9] C.L. Jiang, et al., Phys. Rev. C 81 (2010) 0204611.
[10] A. Shrivastava, et al., Phys. Rev. Lett. 103 (2009) 232702.
[11] C.M. Castaneda, et al., Phys. Lett. B 77 (1978) 371.
[12] H. Utsunomiya, et al., Phys. Rev. C 28 (1983) 1975.
[13] V. Tripathi, et al., Phys. Rev. C 72 (2005) 017601.
[14] J. Wilczynski, et al., Phys. Rev. Lett. 45 (1980) 606;
J.H. Barker, et al., Phys. Rev. Lett. 424 (1980) 45.
[15] Yu.E. Penionzhkevich, et al., J. Phys. G: Nucl. Part. Phys. 36 (2009) 025104.
[16] I.J. Thompson, A. Diaz-Torres, Prog. Theor. Phys. Suppl. 154 (2004) 69.
[17] P.P. Singh, et al., Phys. Rev. C 80 (2009) 064603.
[18] J. Mierzejewski, et al., Phys. Scr. T 150 (2012) 014026.
[19] H. Helppi, et al., Phys. Rev. C 23 (1981) 2345.
[20] D. Mertin, et al., Nucl. Phys. A 301 (1978) 365.
[21] H.-E. Mahnke, G. Kaindl, F. Bacon, D. Shirley, Nucl. Phys. A 247 (1975) 195.
[22] A. Shrivastava, et al., Phys. Lett. B 633 (2006) 463.
[23] G.D. Dracoulis, et al., J. Phys. G: Nucl. Part. Phys. 23 (1997) 1191.
[24] A. Shrivastava, et al., in: Ch. Schmitt, A. Navin, M. Rejmund, D. Lacroix, H. Goutte (Eds.), Proc. Int. Conf. FUSION11, Saint-Malo, France, 2–6 May 2011, EPJ Web of Conferences, vol. 17, 2011, p. 03001.
[25] A. Diaz-Torres, Comput. Phys. Commun. 182 (2011) 1100.
[26] A. Gavron, Phys. Rev. C 21 (1980) 230.
[27] L.C. Chamon, et al., Phys. Rev. C 66 (2002) 014610.
[28] D.H. Luong, et al., Phys. Lett. B 695 (2011) 105.
[29] R. Broglia, A. Winther, Heavy Ion Reactions, vol. 84, Addison–Wesley, Redwood City, CA, 1991.
[30] A. Jungclaus, et al., Phys. Rev. C 66 (2002) 014312;
R.M. Clark, et al., Phys. Rev. C 72 (2005) 054605.